J Fluoresc (2015) 25:1183–1189
DOI 10.1007/s10895-015-1605-2

ORIGINAL ARTICLE

Characterization of the Aggregation-Induced Enhanced Emission of *N*,*N*′-bis(4-methoxysalicylide)benzene-1,4-diamine

Fuyong Wu[1] · **Guangjun Xu**[1] · **Xi Zeng**[1] · **Lan Mu**[1] · **Carl Redshaw**[2] · **Gang Wei**[3]

Received: 21 January 2015 / Accepted: 30 June 2015 / Published online: 14 July 2015

Abstract *N*,*N*′-bis(4-methoxysalicylide)benzene-1,4-diamine (**S1**) was synthesized from 4-methoxysalicylaldehyde and *p*-phenylenediamine and it was found to exhibit interesting aggregation-induced emission enhancement (AIEE) characteristics. In aprotic solvent, **S1** displayed very weak fluorescence, whilst strong emission was observed when in protic solvent. The morphology characteristics and luminescent properties of **S1** were determined from the fluorescence and UV absorption spectra, SEM, fluorescence microscope and grading analysis. Analysis of the single crystal diffraction data infers that the intramolecular hydrogen bonding constitutes to a coplanar structure and orderly packing in aggregated state, which in turn hinders intramolecular C-N single bond rotation. Given that the three benzene rings formed a large plane conjugated structure, the fluorescence emission was significantly enhanced. The absolute fluorescence quantum yield and fluorescence lifetime also showed that radiation transition was effectively enhanced in the aggregated state. Moreover, the AIEE behavior of **S1** suggests there is a potential application in the fluorescence sensing of some volatile organic solvents.

Keywords Salicylaldehyde derivative · Aggregation-induced emission enhancement · Fluorescence probe · Volatile organic solvent

Electronic supplementary material The online version of this article (doi:10.1007/s10895-015-1605-2) contains supplementary material, which is available to authorized users.

✉ Lan Mu
sci.lmou@gzu.edu.cn

✉ Gang Wei
gang.wei@csiro.au

[1] Key Laboratory of Macrocycle and Supramolecular Chemistry of Guizhou Province, Guiyang 550025, China

[2] Department of Chemistry, University of Hull, Hull HU6 7RX, UK

[3] CSIRO Manufacturing Flagship, PO Box 218, Lindfield, NSW 2070, Australia

Introduction

Although many organic luminescent molecules exhibit good luminescence properties in solution, their fluorescence decreases or is quenched when aggregation occurs or in the solid state [1], which limits the application of these molecules in thin films and the solid state. The problem of fluorescence quenching of some organic luminescence molecules need to be solved to allow for their efficient use in solid devices. More highly efficiency, stable and multi-colored organic light-emitting materials need to be developed [2, 3]. A series of aggregation induced enhanced emission (AIEE) compounds have been reported by the Tang et al. [4, 5], and more of these AIEE compounds have been found including styrene acrylic instead of nitrile [6, 7], salicylaldehyde [8–10] and coumarin-based Schiff bases [11] etc. Our group has also reported AIEE compounds based on phenothiazine [12] or naphthalene [13] as the structural units. AIEE mechanisms including restriction of intermolecular rotation, formation of J-aggregates, blockage of non-radiative relaxation pathways of the excited species, intramolecular planarization inhibition of photoisomerization and photocyclization have been proposed [14–18]. Organic compounds, which possess the characteristics of AIEE via changing of the molecular coplanarity, increasing the rigid conjugate structure, conformational change and orderly accumulation under the conditions of aggregation or in the solid state, have excellent prospects for application in organic luminous materials, chemical and biological sensors and so on.

Herein, we report *N*,*N*′-bis(4-methoxysalicylide)benzene-1,4-diamine (**S1**), which has been readily synthesized in a one step condensation reaction using 4-methoxysalicylaldehyde and *p*-phenylenediamine. The cyclic structure was formed by intermolecular hydrogen bonding between the Schiff base nitrogen atoms and the hydroxyl group of the benzene, which not only increases the molecular planarity, but also limits the intramolecular rotation around the single bond involving the carbon and nitrogen. Luminous efficiency can be improved through the formation of large coplanar and conjugated cyclic structures. The aggregation and the high-efficiency photoluminescence in the solid state have been investigated.

Experimental

Materials and Methods

All chemicals used in this work, including phenylenediamine, ethanol, dimethyl sulfoxide, *p*-methoxy salicylaldehyde and β-cyclodextrin were purchased directly from chemical suppliers (Aladdin Chemical Reagent Co., Ltd., China) and were used without further purification. The cucurbit[*n*]urils (Q[*n*]s *n*=5, 6, 7, 8) were made in our own laboratory [19, 20]. All reagents were of analytical grade. Doubly-distilled water was used in all of the experiments.

Fluorescence spectra were recorded on a Cary Eclipse fluorescence spectrophotometer (Varian) equipped with a xenon discharge lamp. Absorbance spectra were recorded on a TU-1901 spectrophotometer (Beijing General Instrument Co., China). Single crystal X-ray diffraction studies were conducted on a Smart CCD Apex2 diffractometer (Bruker). Fluorescence images of the microcrystals were obtained by a C-SHGL fluorescence microscope (Nikon) with an inverted fluorescence micro-manipulation system. Suspensions were obtained using a TGL-16GA centrifuge (Shangdong Xing Ke Intelligent Technology Co., Ltd., China). Scanning electron microscopy (SEM) images were recorded on a KYKY-2800B microscope (Beijing Branch Instrument Co., Ltd., China). The size distribution was determined by Nano ZS nanoparticle zeta potentiometer (Melvin British Co., UK). The fluorescence lifetimes and absolute fluorescence quantum yields were detected by a FLS920 steady/transient state fluorescence spectrophotometer (Edinburgh Instruments Co., UK) with an electric refrigeration photomultiplier tube detector, 375 nm excitation wavelength, with laser output pulse width 90 ps.

The Synthesis of Compound **S1**

The synthesis of compound **S1** was performed according to the literature [21] and was verified by ^{1}H NMR spectroscopy (Supporting Information, Fig. S1).

Single Crystal X-ray Crystallography of **S1**

A single crystal of **S1** was grown by slow crystallization from a solution in THF and a small amount of MeOH. X-ray data were collected on a Smart ApexII CCD diffractometer, the crystal structure determination and analytical methods were the same as reported previously [22].

Preparation of **S1** *for SEM and Fluorescence Images*

A 50 μM solution of **S1** in DMSO/ H_2O (Vol. 80 % H_2O) was added to a 25 mL flask, and a suspension was obtained by centrifugation. The preparation of samples for SEM involved applying a few drops of a suspension to a glass slide, which was covered with a black film. After drying at room temperature, the prepared samples were sputter-coated with gold/palladium. Samples for fluorescence microscopy were prepared by applying a few drops of a suspension to a glass slide and then covering with a coverslip.

Results and Discussion

Molecular Structure

Crystallographic data for **S1** have been deposited with the Cambridge Crystallographic Data Centre (CCDC-906106). Copies of the data can be obtained on application to the CCDC, 12 Union Road, Cambridge CB2 1EZ, UK [fax: + 4401223 762911 or kamila@ccdc.cam.ac.uk].

The crystal structure of **S1** belongs to the monoclinic crystal system; X-ray diffraction measurements and the experimental details for the structure analysis of **S1** are given in Table 1.

AIEE Property of S1

S1 can readily be dissolved in aprotic polar solvents such as DMSO, THF or DMF, but cannot be dissolved in the protic solvents MeOH, EtOH or H_2O. The fluorescence spectra revealed that upon excitation of a dilute DMSO solution of **S1** (10 μM) at 379 nm, a weak fluorescence emission was observed. However, the fluorescence intensity increased continuously when 60~80 % volume fractions of H_2O were added to the DMSO solution, whilst the max emission wavelength underwent a blue-shift on addition of water (Fig. 1a). When compared with the use of the DMSO solvent, there was a five times increase of fluorescence intensity at 510 nm when the H_2O volume fraction increased up to 80 % in the DMSO/ H_2O mixture solvent. On the contrary, the maximum absorption at 380 nm decreased with the addition of H_2O to the DMSO/ H_2O mixture solvent (Fig. 1b). The AIEE phenomenon can be

Table 1 Crystallographic data and structure refinements for S1

Empirical formula	$C_{22}H_{20}N_2O_4$	θ range, (°)	$3.32 \le \theta \le 26.00$
Formula weight	376	Absorption coefficient/mm^{-1}	0.114
Temperature(K)	293(2)	F(000)	876
Crystal system	monoclinic	Reflections collected	24,075
Space group	C_2/C	Independent reflections	3240
a/Å	25.873(8)	Observed reflections[$I>2\sigma(I)$]	1472
b/Å↩	6.257(2)	Refinement method	Full-matrix least squares on F^2
c/Å	12.323(4)	Number of parameters	139
α/(°)	90	Goodness-of-fit F^2	0.753
β/(°)	113.817	Final R indices[$I>2\sigma(I)$]	R_1=0.0661, ωR_2=0.1610
γ/(°)	90	Rindices (all data)	R_1=0.0728, ωR_2=0.1766
Volume/nm^3	3684.6(13)	Final weighting scheme	$\omega=1/[\sigma^2(F_0^2)]+(0.1791P)^2+0.9809P)$, $P=[F_0^2+2F_c^2]/3$
Z	3	$(\Delta\rho)_{max}$/(e nm^{-3})	0.210
D_{calc}/(g cm)	1.541	$(\Delta\rho)_{min}$/(e nm^{-3})	−0.598

seen directly from the fluorescence spectral changes, and indicated the formation of aggregates in protic solvent [23].

Usually, the formation of aggregates can be observed in suspensions made by centrifugal concentration [24]. The fluorescence of **S1** aggregates in DMSO/ H_2O mixed solvent was supported by observation using fluorescence microscopy. Figure 2a shows photographs of **S1** in different solvents and in the solid state at 365 nm UV illumination. No obvious fluorescence was observed in DMSO solvent (Fig. 2a (a)), but strong bright yellow-green fluorescence was observed in the DMSO/ H_2O (Vol. 80 % H_2O) solvent mixture (Fig. 2a (b)), and a yellow-green color appeared on production of powdered **S1** (Fig. 2a (c)). Fluorescence microscopy of **S1** powder also revealed strong yellow-green fluorescence (Fig. 2b), indicating aggregates of **S1** in the mixed solvent and the solid-state for **S1**; both have the same fluorescence emission.

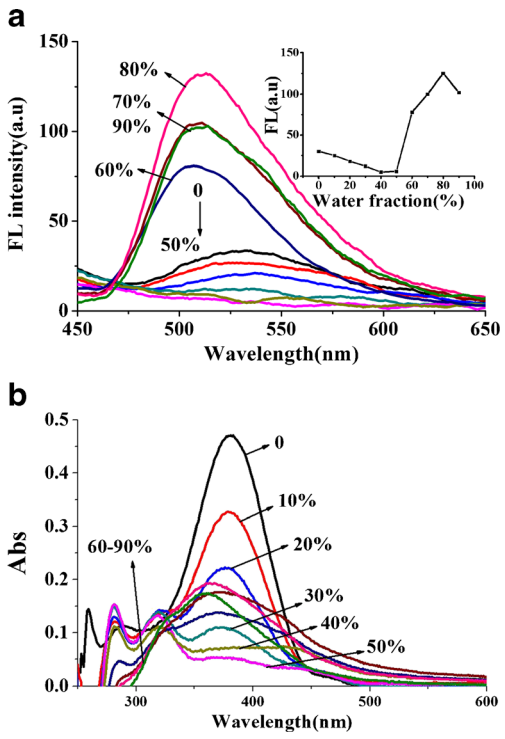

Fig. 1 Fluorescence (**a**) and UV absorption spectra (**b**) of **S1** (10 μM) in a DMSO/ H_2O solvent mixture. Inset: the variation of emission intensity of **S1** with increasing water fraction in DMSO/ H_2O mixture solvent. λ_{ex} / λ_{em}=379 / 510 nm

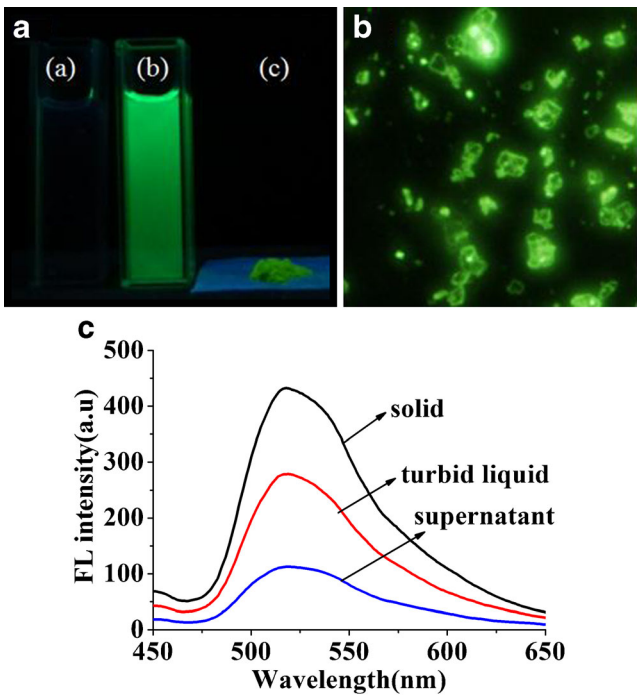

Fig. 2 **a** Photos of **S1** (10 μM) solution in DMSO (*a*), in DMSO/ H_2O (Vol. 80 % H_2O) mixed solvent (*b*) and **S1** powder (*c*) under 365 nm UV light; **b** **S1** powder under the fluorescence microscopy; **c** Fluorescence spectra of **S1** in different forms. *a*. solid; *b*. turbid liquid; *c*. supernatant. λ_{ex}=379 nm

Furthermore, the fluorescence spectra of **S1** were obtained from a turbid liquid: the supernatant from centrifugation of the solution in DMSO/ H_2O, and the solid state (Fig. 2c), which validated that the measured spectra originated from the same luminophore, regardless of whether in the solid state or dispersed in solution.

The size distribution of **S1** in different volume fractions of DMSO/ H_2O mixed solvent were investigated by nanoparticle zeta potentiometry (Fig. 3). When the volume fractions of DMSO were higher than 50 %, the **S1** molecules tended to be distributed in the solution, and no nanoparticles were detected; when the volume fraction of aprotic solvent (DMSO) was reduced to 40 %, particle size analysis revealed that there were 100~380 nm sized molecular aggregates present, *ie* their proportion increased with increasing protic solvent (H_2O); When the volume fractions of DMSO was reduced to 10 %, the particle size of the aggregates was in the range 100~700 nm, most of which were about 200~300 nm. On decreasing of the DMSO volume fractions, the proportion of the large sized aggregates increased. This strongly suggested that the molecules of **S1** existed in the form of aggregates rather than a precipitate in an appropriate ratio of a DMSO/H_2O solvent mix. The particle size distribution and intensity of the molecular aggregates were controlled by the proportion of protic and aprotic solvent.

The solution of **S1** in DMSO/H_2O (Vol. 80 % H_2O) mixed solvent was separated by centrifugation. An SEM image (Fig. 4a) and a fluorescence microscopy image (Fig. 4b) of the centrifuged suspension showed a nanoparticle morphology (approx. 1.44 μm) and the bright yellow-green colored nanoaggregates.

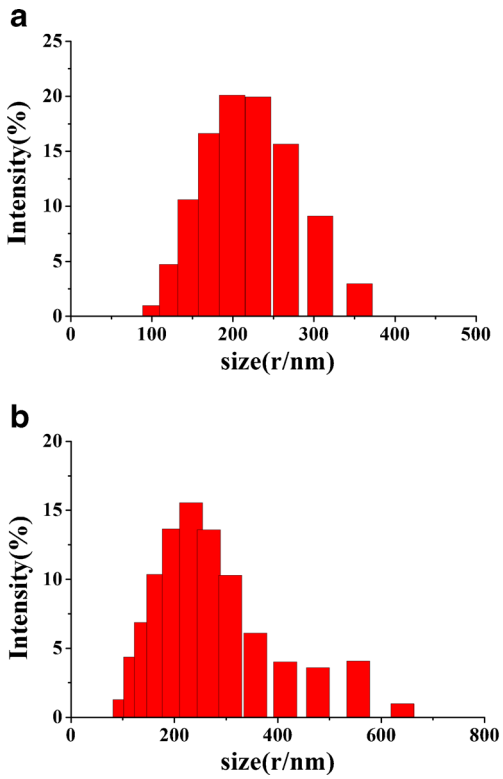

Fig. 3 Intensity changes of size distribution of **S1** (10 μM) in DMSO/ H_2O mixed solvent. **a** Vol. 60 % H_2O; **b** Vol. 90 % H_2O

Investigation of the Characteristic Mechanism of AIEE

The crystal structure of **S1** can help to explain the mechanism of the AIEE phenomenon by analysis of the geometrical parameters. In Fig. 5(a), the angles of C(8)-N(1)-C(10), N(1)-C(8)-C(1), C(11)-C(10-N(1) and C(9)-C(10)-N(1) were determined as 120.92(15)°, 121.90(16)°, 123.57(15)° and 117.60(15)°, respectively; the torsion angles of C(1a)-C(8a)-N(1a)-C(10a) and C(1)-C(8)-N(1)-C(10), were determined as 176.42°, 175.67°, respectively, *ie* close to 180° planar angle. The dihedral angle of 0.8° proved that A and B were coplanar rings. H(1) and N(1) formed a bond length of 2.596(2) Å for the intramolecular hydrogen bonding, and this not only enlarged the conjugated plane structure of the **S1** molecule form five rings, but also formed a stable six-membered ring from "-C(8)=N(1)…H(1)-O(1)-C(6)=C(1)-", thereby ensuring intramolecular rotation was allowed only about the C-N single bond. In DMSO solvent, the **S1** molecules were in the dispersion state, so for the two symmetric coplanar rings, both sides of the middle benzene ring, rotated freely around the single bond of C(10)-N(1) or C(10a)-N(1a), and it was difficult for them to adopt a coplanar rigid structure. Hence, most of the excited-state energy was lost, and the fluorescence emission was very weak. In the DMSO/H_2O mixed solvent, aggregation of the **S1** molecules occurred, and the distance between the molecules was reduced; the free rotation weakened, and therefore the coplanarity was enhanced. As shown in Fig. 5(b), the distance was only 3.8492 Å from the C(E) ring to the D(F) ring, and the molecules were able to adopt a stagger intermolecular π-π parallel stacked arrangement, which lead to rapid fluorescence enhancement; this is consistent with the literature [25, 26]. With the foregoing spectroscopic observations, the fluorescence intensity increases means the intramolecular planarization enhanced in the excited state, and the absorption decreases means the intramolecular planarization decreases in the ground state.

This AIEE effect could be explained by the blocking of the non-radiative intramolecular rotational decay of the excited

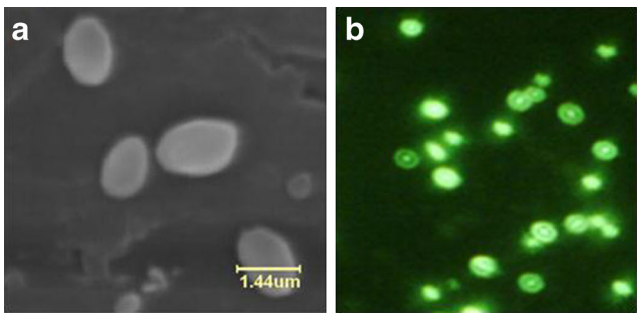

Fig. 4 SEM image (**a**) and fluorescence microscopy image (**b**) turbid liquid of **S1** (50 μM) in DMSO/ H_2O (Vol. 80 % H_2O)

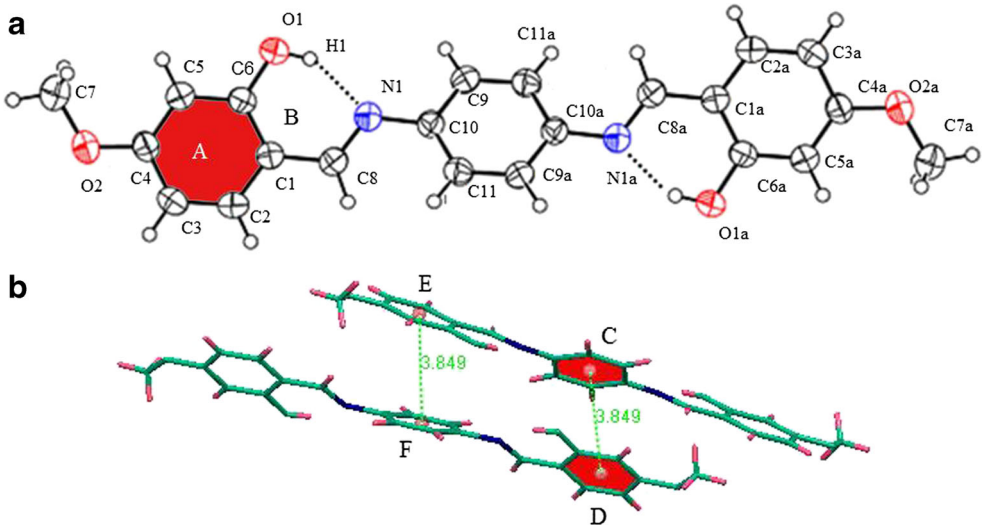

Fig. 5 Molecular structure of **S1** (**a**), the details of π-π interaction (**b**)

molecules through the formation of aggregates [8, 23, 27], due to the restricted motion of **S1** in the mixed solvent. The effect of **S1** the concentration was studied in different volume fractions of DMSO/ H_2O mixed solvent (Supporting Information, Fig. S2). When the concentration of **S1** was as low as 1 μM, there was no fluorescent enhancement, even if the volume of H_2O reached 40 %~90 %, it was difficult to form aggregates at such low concentrations. Furthermore, the explanation is supported by the fluorescent enhancement of **S1** as the viscosity of solvent (glycol) increased (Supporting Information, Fig. S3 and Table 1), given that high viscosity would inhibit intramolecular rotation and induce the AIEE effect. However, clear variations were observed up to an appropriate concentration (100 μM) when the volume of H_2O reached 40 %; the ordered stacking of aggregates is effective in limiting the intramolecular rotation. The changes of fluorescence intensity of **S1** in DMSO/ H_2O (10 μM, Vol. 80 % H_2O) at different temperatures were investigated (Supporting Information, Fig. S4 and Table 2), and it was found that the fluorescence intensity decreased on increasing the temperature; rotation is more facile at higher temperatures even in the state of aggregation. At 70 °C, the fluorescence intensity of the aggregated state decreased to the same as in pure DMSO.

The luminescence properties of **S1** (10 μM) versus different cavities of various macrocyclic compounds was investigated. In Fig. 6, **S1** is shown to exhibit weak fluorescence emission in DMSO/ H_2O (Vol. 10 % H_2O) solution due to being in the dispersed state, but exhibits high selectivity for Q[6] over other Cucurbit[*n*]urils (Q[*n*]s *n*=5, 7, 8) and β-cyclodextrin (β-CD) with fluorescence enhancement, while other macrocyclic molecules did not exhibit this phenomenon, including Q[5]s, Q[7]s, Q[8]s, β-CD. This may be attributed to complementary space matching that allows the **S1** molecules to just enter into the hydrophobic cavity of Q[6], which provide a microenvironment for the luminescence molecule, thereby limiting free rotation of the intramolecular single bond, and reducing the non-radiative transition, resulting in fluorescence enhancement. This phenomenon is similar to the aggregated state in protic solvent (DMSO/ H_2O).

All of the above results indicate that **S1** is an AIEE molecule, for which free intramolecular rotation of the fluorophore can be inhibited on going from the dispersed state to the aggregated state. The clear AIEE phenomenon of **S1** was observed up to an appropriate concentration, solvent, microenvironment and temperature. The enhanced emission of the **S1** solution is attributed to the combined effects of molecular planarization, ordered stacking, and inhibition of the intramolecular rotation.

Table 2 Fluorescence lifetime change of S1 in different solvent system

Solvent	DMSO/H_2O			THF/H_2O		
Vol. H_2O (%)	40	60	80	40	60	80
τ/ns	3.03	3.64	4.92	2.93	3.33	3.89

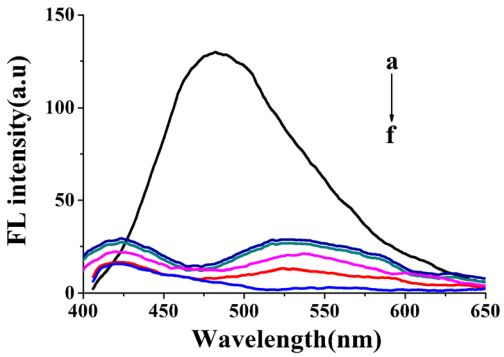

Fig. 6 Fluorescence spectra of **S1** in DMSO/ H_2O (10 μM, Vol. 10 % H_2O) upon the addition of different macrocyclic molecules. *a*. Q[6]; *b*. **S1**; *c*. Q[7]; *d*. Q[5]; e. Q[8]; *f*. CD. λ_{ex}=379 nm

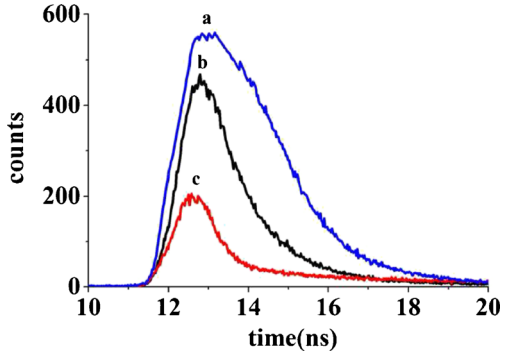

Fig. 7 Transient luminescence decays curves of **S1** in the DMSO/ H_2O mixture solution. *a*. Vol. 80 % H_2O; *b*. Vol. 60 % H_2O; *c*. Vol. 40 % H_2O

The fluorescence lifetime of **S1** in various organic solvents and different volume fractions of mixed solutions were determined by a steady/transient state fluorescence spectrophotometer, respectively. The transient luminescence decay curves of **S1** are shown in Fig. 7. The longest fluorescence lifetime is 4.92 ns in DMSO/ H_2O (Vol. 80 % H_2O) solution with 1.201 goodness of fit (Table 2), and an absolute fluorescence quantum yield (Φ=0.18) measured with an integrating sphere attachment. In the same solvent, the fluorescence lifetimes of **S1** were enhanced on increasing the water volume fraction, due to an increase of aggregation in the protic solvent, which contributes to the orderly accumulation of molecules, and luminous efficiency enhancement. The fluorescence lifetime is slightly different in different solvents, but the variation is small. The merits of strong emission and long emission lifetimes may qualify **S1** as a highly attractive candidate for organic luminescent molecules that can be used in the solid or the aggregated state.

Utilizing the AIEE property for the detection of volatile organic solvent has been reported [28]. Hereon, **S1** as a fluorescence detection reagent in the solid/ dispersed state was also investigated. THF was selected as the test solvent given its strong volatility and aprotic solvent of **S1**. A THF solution containing a small amount of **S1** was dripped onto a thin-layer chromatography (TLC) plate, whilst observing the spot of TLC plate under 365 nm ultraviolet light at room temperature. The spot exhibited yellow-green fluorescence after evaporating off the THF solvent (Fig. 8a), and the yellow-green fluorescence spot disappeared under a vapor of THF in a petri dish which contained a small amount of THF solvent (Fig. 8b). The yellow-green fluorescence spot was observed again under ultraviolet light, and then the THF solvent of the TLC plate was evaporated (Fig. 8c), *ie* this is a reversible process. There is thus the potential of utilizing **S1** as a sensor for volatile organic solvents.

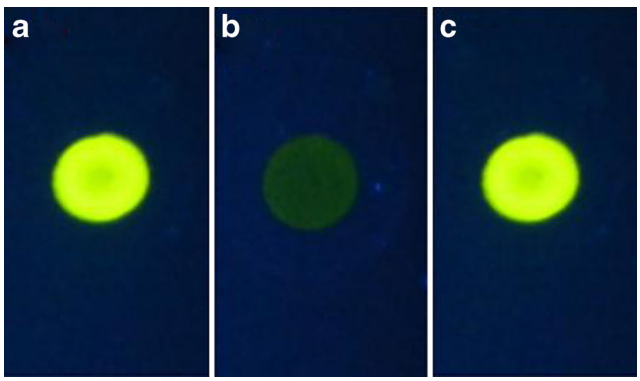

Fig. 8 Photos of the spots of **S1** on the TLC plates placed in the petri dish sets **a** without and **b** with THF vapor, **c** take away the solvent-vapor under 365 nm UV light

Conclusions

The simple salicylaldehyde derivative **S1** was synthesized readily in one step by condensation of 4-methoxy salicylaldehyde with p-phenylenediamine. The AIEE characteristics of **S1** were investigated in DMSO/H_2O solution by fluorescence spectroscopy. The absolute fluorescence quantum yields and the fluorescence lifetimes of **S1** in different solvents revealed that it was an excellent luminescent solid and also in the aggregated state. The AIEE phenomenon may be attributed to the combined effects of intramolecular planarization, the presence of intermolecular π-π interactions and intermolecular ordered aggregation, all of which reduce the non-radiative transition in the aggregated state. Furthermore, utilizing the reversible luminescence features of **S1** in the solid or dispersed state allows for the detection of volatile organic solvents.

Acknowledgments We are grateful for the financial support from the Natural Science Foundation of China (No. 21165006), the Fund of the International cooperation projects of Guizhou Province (No. 20137002) and "Chun-Hui" Fund of Chinese Ministry of Education (No. Z2011033, Z2012053). The EPSRC is thanked for financial support (Overseas Travel award to CR).

References

1. Song PS, Chen XT, Xiang Y, Huang L, Zhou ZJ, Wei RR, Tong AJ (2011) A ratiometric fluorescent pH probe based on aggregation-induced emission enhancement and its application in live-cell imaging. J Mater Chem 21:13470–13475
2. Li HY, Chi ZG, Xu BJ, Zhang XQ, Li XF, Liu SW, Zhang Y, Xu JR (2011) Aggregation-induced emission enhancement compounds containing triphenylamine-anthrylenevinylene and tetraphenylethene moieties. J Mater Chem 21:3760–3767
3. McGehee MD, Heeger AJ (2000) Semiconducting (conjugated) polymers as materials for solid-state lasers. Adv Mater 12:1655–1668
4. Liu Y, Tang YH, Nikolay NB et al (2010) Fluorescent chemosensor for detection and quantitation of carbon dioxide gas. J Am Chem Soc 132:13951–13953
5. Chen JW, Charles CWL, Jacky WYL, Dong YP, Samuel MFL, Ian DW, Zhu DB, Tang BZ (2003) Synthesis, light emission,

nanoaggregation, and restricted intramolecular rotation of 1,1-substituted 2,3,4,5-tetraphenylsiloles. Chem Mater 15(7):1535–1546
6. An BK, Lee DS, Park SY (2004) Strongly fluorescent organogel system comprising fibrillar self-assembly of a trifluoromethyl-based cyanostilbene derivative. J Am Chem Soc 126:10232–10233
7. An BK, Kwon SK, Park SY (2007) Photopatterned arrays of fluorescent organic nanoparticles. Angew Chem Int Ed 46:1978–1982
8. Tang WX, Xiang Y, Tong AJ (2009) Salicylaldehyde azines as fluorophores of aggregation-induced emission enhancement characteristics. J Org Chem 74:2163–2166
9. Chen XT, Xiang Y, Li N, Song PS, Tong AJ (2010) Fluorescence turn-on detection of protamine based on aggregation-induced emission enhancement characteristics of 4-(60-carboxyl)hexyloxysalicylaldehyde azine. Analyst 135:1098–1105
10. Chen XT, Wei RR, Xiang Y, Zhou ZJ, Ki L, Song PS, Tong AJ (2011) Organic crystalline solids response to Piezo/thermo stimulus: donor acceptor (DA) attached salicylaldehyde azine derivatives. J Phys Chem C 115:14353–14359
11. Xiao HD, Chen K, Cui DD, Jiang NN, Yin G, Wang J, Wang RY (2014) Two novel aggregation-induced emission active coumarin-based Schiff bases and their applications in cell imaging. New J Chem 38:2386–2393
12. Cao X, Zeng X, Mu L, Chen Y, Wang RX, Zhang YQ, Zhang JX, Wei G (2012) Synthesis, characterization and aggregation induced enhanced emission of new phenothiazine hydrazone. Chem J Chin Univ 33(10):2184–2190
13. Cao X, Zeng X, Mu L, Chen Y, Wang RX, Zhang YQ, Zhang JX, Wei G (2013) Characterization of the aggregation-induced enhanced emission, sensing, and logic gate behavior of 2-(1-hydroxy-2-naphthyl)methylene hydrazine. Sensors Actuators B 177:493–499
14. Luo J, Xie Z, Lam JWY, Cheng L, Chen H, Qiu C, Kwok HS, Zhan XW, Liu YQ, Zhu DB, Tang BZ (2001) Aggregation-induced emission of 1-methyl-1,2,3,4,5-pentaphenylsilole. Chem Commun: 1740–1741
15. An BK, Lee DS, Lee JS, Park YS, Song HS, Park SY (2004) Strongly fluorescent organogel system comprising fibrillar self-assembly of a trifluoromethyl-based cyanostilbene derivative. J Am Chem Soc 126:10232–10233
16. Sun Y, Liu Z, Liang X, Fan J, Han Q (2013) Study on photophysical and aggregation induced emission recognition of 1,8-naphthalimide probe for casein by spectroscopic method. Spectrochim Acta A 108:8–13
17. Hong Y, Lam JWY, Tang BZ (2009) Aggregation-induced emission: phenomenon, mechanism and applications. Chem Commun: 4332–4353
18. Hong Y, Lam JWY, Tang BZ (2011) Aggregation-induced emission. Chem Soc Rev 40:5361–5388
19. Kazunobu H, Yasushi M, Tohru M, Keiji M, Hisashi Y (1981) Successive Beckmann rearrangement-alkylation sequence by organoaluminum reagents. A simple route to dl-Pumiliotoxin C. J Am Chem Soc 103:1368–1370
20. Jaheon K, In-Sun J, Soo-Young K, Eunsung L, Jin-Koo K, Shigeru S, Kentaro Y, Kimoon K (2000) New cucurbituril homologues: syntheses, isolation, characterization, and x-ray crystal structures of cucurbit[n]uril (n=5, 7, and 8). J Am Chem Soc 122:540–541
21. Görner H, Khanra S, Weyhermüller T, Chaudhuri P (2006) Photoinduced intramolecular proton transfer of phenol-containing ligands and their zinc complexes. J Phys Chem A 110:2587–2594
22. Zhang LF, Zhao JL, Mu L, Xue SF, Tao Z, Wei G (2010) Synthesis of pheyl-acetylacetone rhodamine B derivative and recognition properties for Fe^{3+}. Chin J Inorg Chem 26(10):1796–1803
23. An BK, Kwon SK, Jung SD, Park SY (2002) Enhanced emission and its switching in fluorescent organic nanoparticles. J Am Chem Soc 124:14410–14415
24. Tang BZ, Geng Y, Lam JWY, Li B, Jing X, Wang X, Wang F, Pakhomov AB, Zhang XX (1999) Processible nanostructured materials with electrical conductivity and magnetic susceptibility: preparation and properties of maghemite/polyaniline nanocomposite films. Chem Mater 11:1581–1589
25. Feng X, Tong B, Shen JB, Shi JB, Han TY, Chen L, Zhi JG, Lu P, Ma YG, Dong YP (2010) Aggregation-induced emission enhancement of aryl-substituted pyrrole derivatives. J Phys Chem B 114:16731–16736
26. Qian Y, Li SY, Zhang GQ, Wang Q, Wang SQ, Xu HJ, Li CZ, Li Y, Yang GQ (2007) Aggregation-induced emission enhancement of 2-(2′-Hydroxyphenyl)benzothiazole-based excited-state intramolecular proton-transfer compounds. J Phys Chem B 111:5861–5868
27. Oelkrug D, Tompert A, Gierschner J, Egelhaaf H, Hanack M, Hohloch M, Steinhuber E (1998) Tuning of fluorescence in films and nanoparticles of oligophenylenevinylenes. J Phys Chem B 102:1902–1907
28. Hong YN, Lam JWY, Tang BZ (2009) Aggregation-induced emission: phenomenon, mechanism and applications. Chem Commun: 4332–4353